

Orbital differentiation and the role of orbital ordering in the magnetic state of Fe superconductors

E. Bascones,^{*} B. Valenzuela,[†] and M.J. Calderón[‡]

Instituto de Ciencia de Materiales de Madrid, ICM-CONIC, Cantoblanco, E-28049 Madrid (Spain).

(Dated: August 10, 2012)

We analyze the metallic $(\pi, 0)$ antiferromagnetic state of a five-orbital model for iron superconductors. We find that with increasing interactions the system does not evolve trivially from the pure itinerant to the pure localized regime. Instead we find a region with a strong orbital differentiation between xy and yz , which are half-filled gapped states at the Fermi level, and itinerant zx , $3z^2 - r^2$ and $x^2 - y^2$. Orbital ordering arises as a consequence of the interplay of the exchange energy in the antiferromagnetic x direction due to yz localization and the kinetic energy gained by the itinerant orbitals along the ferromagnetic y direction with an overall dominance of the kinetic energy gain. We argue that iron superconductors are close to the boundary between the itinerant and the orbital differentiated regimes and that it could be possible to cross this boundary with doping.

PACS numbers: 75.10.Jm, 75.10.Lp, 75.30.Ds

There is a strong interrelation between the orbital degree of freedom, the magnetization, and the lattice structure in the Fe-superconductors. Unveiling the nature of these connections would define the landscape from which superconductivity emerges in these materials. One of the important issues is the determination of the strength of the interactions. Unlike the cuprates, which are antiferromagnetic Mott insulators when undoped, the Fe-superconductors are antiferromagnetic metals, highlighting the relevance of the itinerancy of the conduction electrons. Undoped materials have to accommodate six electrons in the five Fe-d orbitals, with an average filling of 1.2, close to the one of doped Mott insulators.¹⁻³ The itinerant⁴⁻⁷ versus localized^{8,9} origin of the magnetization has been discussed since the discovery of superconductivity in these systems.

On the other hand there is an increasing evidence for orbital differentiation and a possible coexistence of itinerant and localized electrons.¹⁰⁻¹² Angle Resolved Photoemission Spectroscopy (ARPES) measurements report different renormalization values for the various bands close to the Fermi energy depending on their orbital character.^{13,14} Similar qualitative conclusions may be inferred from Dynamical Mean Field Theory (DMFT) and slave-spin calculations.^{1,15-17}

The possible role of orbital ordering in the magnetism is of present interest. The current debate is focused on whether it is the leading instability driving the magnetism¹⁸ or it appears as a consequence of the magnetic ordering,¹⁹⁻²¹ as well as its possible relation to the observed anisotropic properties.^{16,22-33} In particular, the resistivity in the $(\pi, 0)$ antiferromagnetic state was measured to be larger in the ferromagnetic y -direction than in the antiferromagnetic x -direction^{22,23} with a change in sign upon hole doping.³⁴

In order to shed light on the role of the different orbitals on the magnetic state of Fe-superconductors, we analyze the metallic $(\pi, 0)$ antiferromagnetic state as a function of the interactions treated within mean-field.

Close to the non-magnetic phase boundary, electrons are itinerant. An $S = 2$ state compatible with a localized $J_1 - J_2$ description is found deep in the insulating regime.²⁰ With increasing interactions the system does not evolve trivially from the pure itinerant to the pure localized regime. Instead we find a region with a strong orbital differentiation, see Fig. 1. In this region, zx , $3z^2 - r^2$ and $x^2 - y^2$ are itinerant while xy and yz are half-filled and have a gap at the Fermi level. These gapped states are reminiscent of the localized electrons discussed in the literature^{10-12,35} and for simplicity we refer to them as localized. At large values of Hund's coupling the itinerant electrons are also gapped at half-filling while keeping a finite density at the Fermi level. We uncover the different role that orbitals play in the stabilization of the orbital ordering and consequently of the $(\pi, 0)$ antiferromagnetic state. We find that while superexchange¹⁹ between the localized orbitals contributes to generate orbital ordering between yz and zx , it is necessary to invoke the kinetic energy gain of the itinerant electrons along the ferromagnetic direction to describe the observed features. We analyze this result in connection with the resistivity anisotropy.^{24,25} We argue that iron pnictides are close to the boundary between *itinerant* and *strong orbital differentiation* regimes and that it could be possible to cross this boundary with doping.

We consider an interacting two-dimensional five-orbital model for the FeAs layer, as described in Ref. [20]. The Fe orbitals are defined within the one-iron unit cell and hence x and y are given by the Fe-Fe nearest neighbor directions. Only local interactions are included. Interactions with rotational symmetry can be expressed in terms of only two parameters: the intra-orbital Hubbard U and the Hund's coupling J_H .³⁶ We focus on the metallic $(\pi, 0)$ antiferromagnetic state and study the phase diagram as a function of U and J_H/U with interactions treated at the Hartree-Fock level.²⁰

For the tight-binding we use the model described in Ref. [37] and obtained within the Slater-Koster

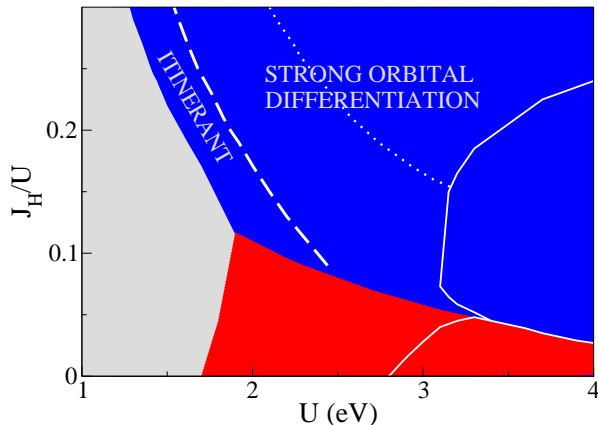


FIG. 1: (Color online) This figure summarizes the main results of this work. The colors distinguish the different $(\pi, 0)$ magnetic phases of the undoped (6 electrons in 5 d orbitals) system as a function of the local interaction parameters U and J_H .²⁰ The grey area is the non-magnetic region. The blue and red areas are magnetic with a high moment (parallel orbital moments) and a low moment (antiparallel orbital moments) state respectively. The white solid lines on the right separate the metallic ($U \lesssim 3$) from the insulating ($U \gtrsim 3$) state. We have analyzed the orbital differentiation within the blue metallic area. We distinguish two different regions that we label, with increasing U , as *itinerant* and *strong orbital differentiation*. The strong orbital differentiation region can be further splitted by the opening of a gap at half-filling, see text for discussion.

formalism³⁸ that takes into account the symmetry of the orbitals and the lattice. In this model the tight-binding parameters are analytic functions of the angle α formed by the Fe-As bond and the Fe plane. The resulting bands, their orbital compositions, the Fermi surface, and the modifications induced by α are all consistent with ab-initio calculations.³⁷ This allows to straightforwardly explore the effect of the Fe-plane lattice structure on the electronic properties. Except when specifically stated, the results are obtained for the undoped case with six electrons per iron $n = 6$, and regular tetrahedra $\alpha = 35.3^\circ$.

The main results of our analysis are summarized in Fig. 1 on top of the $(\pi, 0)$ magnetic phase diagram previously reported in Ref. [20]. The system becomes insulating on the right of the solid white lines. In the grey region the system is not magnetic and the red area corresponds to a low moment state, in which Hund's rule is violated.^{20,39–41} The blue high moment state fulfills Hund's rule. Deep in the insulating regime, this state has a spin $S = 2$ with filled $x^2 - y^2$ and half-filled xy , yz , zx , and $3z^2 - r^2$ [20]. In the region of larger U , an increasing J_H/U leads to metallicity.⁴² We focus here on the metallic blue state, on the left of the solid line. Decreasing the value of U we find different regions which differ on

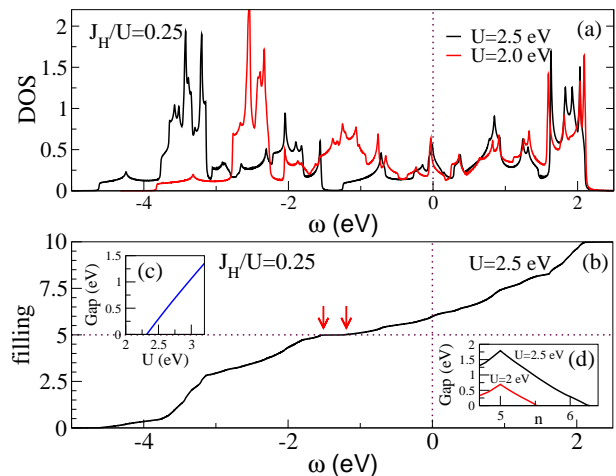


FIG. 2: (Color online) (a) Total density of states for $J_H/U = 0.25$ and $U = 2$ eV (red) and $U = 2.5$ eV (black). The Fermi energy is at $\omega = 0$. For $U = 2.5$ eV, a gap has opened around $\omega \sim -1.5$ eV, which corresponds to half-filling as illustrated in (b), where the integrated density of states (filling) is shown. This opening of a gap at half-filling in the total density of states characterizes the region on the right of the dotted curve within the *strong orbital differentiation* area in Fig. 1. In contrast, there is no gap for $U = 2$ eV. (c) Size of the gap at half-filling as a function of U for $n = 6$. (d) Gap as a function of doping n for the two different values of U . The gap has a maximum at $n = 5$.

their electronic structure and the related orbital differentiation. The regions have been labelled *strong orbital differentiation* and *itinerant*. The nature of the different regions can be inferred from the analysis of the density of states, magnetization and orbital filling curves.

We first focus on the *strong orbital differentiation* region of the phase diagram. Fig. 2 represents the total density of states in two points of this region on both sides of the dotted curve in Fig. 1: $U = 2$ eV and $U = 2.5$ eV, both with $J_H/U = 0.25$ and $n = 6$. In both cases, the system is metallic with no gap at the Fermi level. However, the two curves are qualitatively different with a gap clearly showing below the Fermi energy only for the largest value of U . The opening of this gap in the phase diagram is signaled with a dotted curve in Fig. 1. In Fig. 2(b) it is shown that the gap opens at an energy that corresponds to half-filling (five electrons in the five d orbitals). This gap was found in LDA+U calculations and was associated with a Mott gap.⁴³ This association is compatible with the trends shown by the gap in our Hartree-Fock calculation: It increases upon hole doping (decreasing n) reaching a maximum at $n = 5$ (Fig. 2(d)). Moreover, once this gap opens, its size depends linearly and much stronger on U than the Slater splittings at other energies (Fig. 2(c)).

More can be learned about this *strong orbital differentiation* region by looking at the projection of the density of states on the five Fe d orbitals. The integrated density

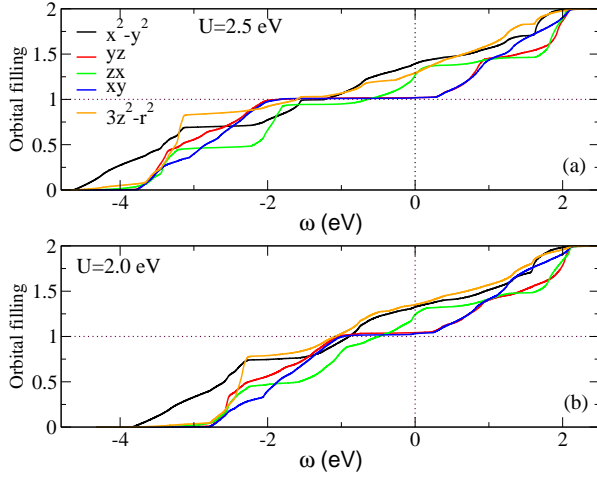


FIG. 3: (Color online) Orbital fillings as a function of energy in the *strong orbital differentiation* regime for (a) $U = 2.5$ eV and (b) $U = 2$ eV. For $U = 2.5$ eV all the orbitals show the gap at negative energies. yz and xy are gapped at the Fermi energy while the other three orbitals are gapped only below the Fermi energy. In contrast, for $U = 2$ eV only two orbitals (yz and xy) show the gap at half-filling while the other three orbitals are itinerant.

of states (filling) of the orbitals as a function of the energy is shown in Fig. 3 for the same two points of the phase diagram as in Fig. 2. The first thing we notice is that for both values of the interaction two orbitals (xy and yz) open their gap at half-filling: their gap is already quite large for $U = 2$ eV and extends up to the Fermi level. The presence of such a large gap pinned at half-filling suggests a localization of xy and yz . This localization is not apparent when looking at the total density of states, Fig. 2. The opening of the gap at negative energies in the total density of states is then related to the appearance of the gap in the other three orbitals zx , $x^2 - y^2$, and $3z^2 - r^2$. However, these three orbitals, unlike xy and yz , remain itinerant in this region, with a finite density of states at the Fermi energy.

The orbital differentiation just discussed is concomitant with orbital ordering: zx tends to be more filled and away from half-filling than yz , which is stuck to half-filling. yz (zx) has a larger intraorbital exchange along the antiferromagnetic x -direction (ferromagnetic y -direction) favoring localization of yz (delocalization of zx) in a magnetic state with $(\pi, 0)$ ordering.¹⁹ This anisotropic exchange comes from the counter-intuitive hoppings relation $|t_{yz,yz}^x| > |t_{yz,yz}^y|$ arising from the combination of direct Fe-Fe and indirect Fe-Pn-Fe hopping amplitudes.³⁷ On the other hand, exchange between xy and yz (zx) is finite only in the ferromagnetic y -direction (antiferromagnetic x -direction) and opposes the localization of yz . As a consequence, as shown in Fig. 4(b), there is more energy gain due to the localization of zx than to the localization of yz for regular tetrahedra ($\alpha = 35.3^\circ$). For elongated tetrahedra ($\alpha > 35.3^\circ$), the localization

of zx becomes much more advantageous in terms of exchange energy, but this does not affect the sign of the orbital ordering in Fig. 4(a). Moreover, the trend changes for smaller values of α , where the localization of yz brings an energy gain, but this is not reflected in the magnitude of the orbital ordering in Fig. 4(a).

A deeper analysis of the orbital dependent hoppings as a function of α helps to clarify the situation. The hoppings involving yz and zx are anisotropic in the plane,^{19,37} see Fig. 4(c). Of those, for a regular tetrahedron ($\alpha = 35.3^\circ$), the largest hoppings in absolute value in the x -direction are $t_{yz,yz}^x$, $t_{yz,x^2-y^2}^x$, $t_{yz,3z^2-r^2}^x$, and $t_{zx,xy}^x$. By symmetry, simply exchanging $yz \leftrightarrow zx$, the largest hoppings in the y -direction are $t_{zx,zx}^y$, $t_{zx,x^2-y^2}^y$, $t_{zx,3z^2-r^2}^y$, and $t_{yz,xy}^y$. From these relations, we see that three orbitals (zx , $x^2 - y^2$, and $3z^2 - r^2$) prefer to be itinerant to gain kinetic energy in the ferromagnetic y -direction. This gain in kinetic energy is maintained when the tetrahedra are elongated while the localization of yz would become even more unfavourable in terms of exchange energy. In squeezed tetrahedra the hopping between zx and $3z^2 - r^2$ along the y -direction strongly decreases and induces a reduction of the orbital ordering. Therefore, the orbital ordering, which does not change sign within the experimentally relevant values of α , see Fig. 4(a), arises due to the interplay of the exchange energy in the x -direction due to yz localization and the kinetic energy in the y -direction due to the itinerancy of zx , $x^2 - y^2$, and $3z^2 - r^2$. Depending on α , these two factors cooperate (squeezed tetrahedra) or compete (regular or elongated tetrahedra), with an overall dominance of the kinetic energy gain. Therefore, this kinetic energy gain is important to stabilize the $(\pi, 0)$ magnetic ordering in the orbital differentiation regime.

The orbital differentiation sustained by the gain in kinetic energy in the y -direction survives upon doping, as shown in Fig. 5. With decreasing n (hole-doping) zx filling decreases fast, changing the sign of the orbital ordering at some point but, remarkably, it is kept away from half-filling, together with $3z^2 - r^2$, even at $n = 5$.⁴⁵

So far, we have discussed the nature of the *strong orbital differentiation* region of the phase diagram in Fig. 1. If we go on decreasing U , xy and yz lose the localization features, getting a finite density of states at the Fermi level, and all carriers are itinerant.

In Fig. 6 (a) the magnetization is depicted as a function of U (black curve) while the evolution of the orbital fillings and their derivatives with U are shown in (b) and (c) respectively. For the values of U with strong orbital differentiation the magnetization has the typical concave shape, but for smaller values of U , the shape of the curve is more complex. xy and yz orbitals are shown to go to half-filling at around the same value of the interactions at which the magnetization becomes concave. Therefore, we estimate the value of the interaction U^* at which xy and yz localize from the change of curvature in the magnetization, which is concave for $U > U^*$. By fitting this concave part, the value of U^* is given by the intercept

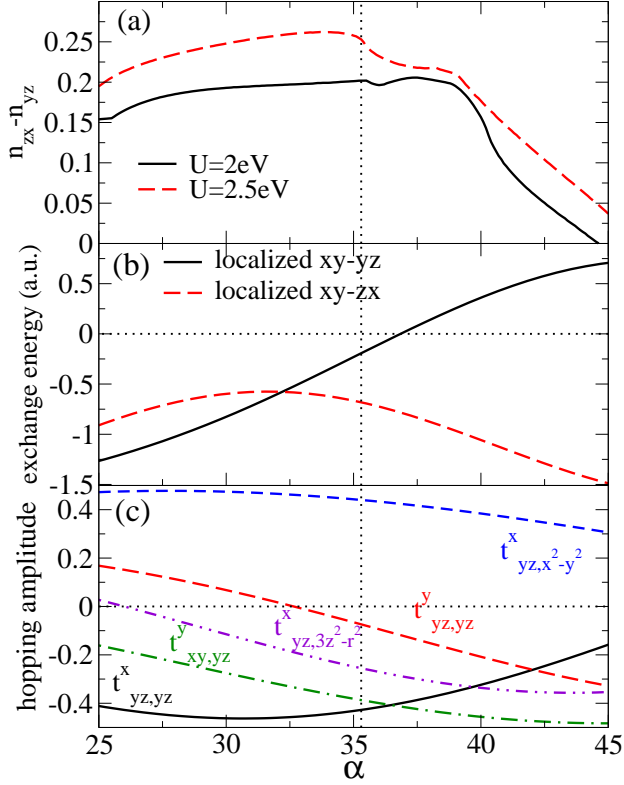


FIG. 4: (Color online) Orbital ordering $n_{zx} - n_{yz}$, exchange energy, and the relevant hopping amplitudes as a function of α , the angle formed by the Fe-As bond and the Fe plane. $\alpha = 35.3^\circ$ (highlighted by a vertical dotted line) corresponds to regular, $\alpha > 35.3^\circ$ to elongated, and $\alpha < 35.3^\circ$ to squeezed tetrahedra. (a) Orbital ordering for different values of U . It gets suppressed with increasing α but it never changes sign within the experimentally relevant values of α . (b) Exchange energy in the $(\pi, 0)$ state due to the localized orbitals and calculated assuming localization of xy and yz (black curve) and localization of xy and zx (red curve). As the tetrahedra elongates, this contribution to the energy would favor a localization of zx versus localization of yz , but this does not happen, see text for discussion. (c) Relevant hopping amplitudes. Note that, by symmetry $t_{zx,zx}^y = t_{yz,yz}^x$, $t_{zx,x^2-y^2}^y = t_{yz,yz}^x$, $t_{zx,x^2-y^2}^z = t_{yz,yz}^x$, etc.³⁷

of the fitting (red-dashed) curve with the x -axes. U^* is represented by a dashed line in Fig. 1.

The derivative of the magnetization displayed in Fig. 6(a) shows two peaks. The second one coincides with the appearance of the concave behavior and the tendency of xy and yz orbitals to half-filling. The first peak is associated with a reorganization of the Fermi surface in the ordered state: below, a spin-density wave between the hole and electron pockets at $(0, 0)$ and $(\pi, 0)$ respectively characterizes the magnetic state, while above, another spin-density-wave instability between the electron pocket at $(0, \pi)$ and the hole pocket at (π, π) gaps this region of the Brillouin zone. This hole pocket is at $(0, 0)$

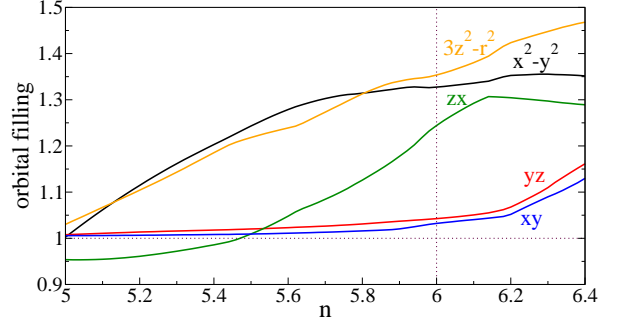


FIG. 5: (Color online) Orbital filling as a function of doping n for $U = 2\text{ eV}$ and $J_H/U = 0.25$. yz and xy are closer to half filling for all dopings. Doping with holes towards $n = 5$ takes all orbitals closer to half-filling but the kinetic energy gain keeps $3z^2 - r^2$ and zx itinerant.

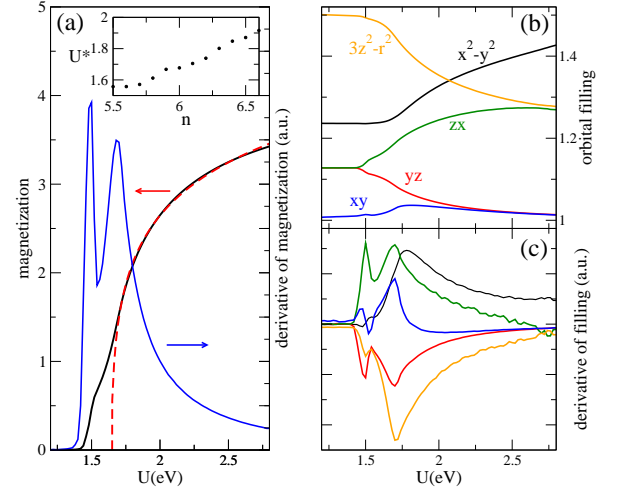


FIG. 6: (Color online) (a) Magnetization (black curve) as a function of the Hubbard parameter U for $J_H/U = 0.25$. Its derivative (blue, in arbitrary units) has two peaks. The red-dashed curve is a fitting to the concave part of the magnetization which is concomitant with the orbital differentiation. The inset shows the values of the U^* at which the magnetization changes from a convex to a concave shape, estimated from the point at which the fitted curve intersects the x -axis. For values of $U < U^*$, the exact shape of the curve depends on the Fe-As-Fe angle and the tight-binding model, see Fig. 7. (b) Orbital fillings versus U and (c) their derivatives. At around U^* , xy , followed by yz , tends to half-filling.

in the 2-Fe Brillouin zone.

Therefore, the detailed behavior of the magnetization in the itinerant region with $U < U^*$ depends on the details of the Fermi surface and the tight-binding model and in particular on the presence or absence of a hole Fermi pocket at (π, π) . To illustrate this, we show in Fig. 7 the dependence of the magnetization on U for our model³⁷ with different values of α , all with a hole Fermi pocket at (π, π) , and for a different tight-binding model⁴⁴ that

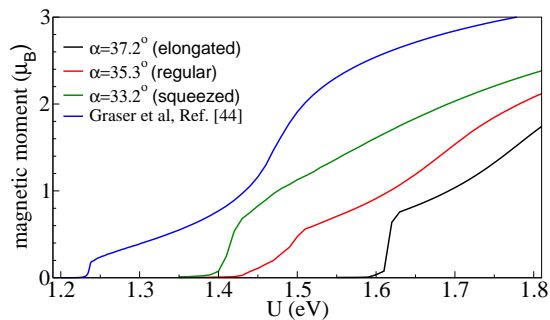


FIG. 7: (Color online) Magnetization versus U for $J_H/U = 0.25$ for different values of the angle α formed by the Fe-As bond with the Fe plane, and for a different tight-binding model reported in Ref. [44]. For sufficiently high values of U , the magnetization recovers a typical concave shape while for the smaller values of U the curves have different shapes.

presents no such Fermi pocket. The Fermi surfaces for these different cases can be found in Refs. [37] and [44], respectively. While both the value of U at which magnetism appears and U^* depend slightly in the model under consideration, the description presented here in terms of itinerant and strong orbital differentiation regimes is valid in all these cases. Moreover the value of the magnetic moment at the crossover is similar for all these models.

In conclusion, we have found that except for small values of the interactions close to the non magnetic boundary, the metallic $(\pi, 0)$ antiferromagnetic state satisfying Hund's rule is characterized by a strong orbital differentiation between half-filled xy and yz orbitals, showing a large gap at the Fermi level and itinerant zx , $3z^2 - r^2$ and $x^2 - y^2$ orbitals away from half-filling and showing a finite density of states at the Fermi level. The large gap at the Fermi level shown by the half-filled orbitals points towards localization. While within the present approach such localization cannot be definitively addressed we believe that it will appear in more elaborate calculations.

The larger tendency to localization of xy agrees with it being close to half-filling in the non-interacting bands and thus very sensitive to interactions, while $3z^2 - r^2$ and $x^2 - y^2$ have the largest filling and thus more itinerant behavior. This result is consistent with Dynamical Mean Field and slave-spin calculations in the paramag-

netic state.^{1,15-17} Moreover, our calculations uncover a strong orbital differentiation between yz and zx , in the antiferromagnetic state where the tetragonal symmetry is broken.

In a previous work, we found orbital ordering to promote a larger conductivity in the ferromagnetic direction except in a striped region of the phase diagram close to the magnetic transition (see Fig. 1(b) in Ref.[24]). This is consistent with the stabilization of the $(\pi, 0)$ magnetic state driven by itinerancy in the y -direction (and the concomitant orbital order) in the region of the phase diagram with both itinerant and gapped carriers.

Current estimates for the interactions⁴⁶ situate the iron superconductors close to the boundary between the *itinerant* and the *strong orbital differentiation* regimes. This is in accord with the values of the magnetic moment that we obtain in this region, expected in our approximation to be similar to those found in LDA calculations.⁵ Moreover, the anisotropy of the conductivity found experimentally in the 122 compounds,^{22,23} which is larger in the antiferromagnetic direction, is consistent with the system not being very deep in the orbital differentiated regime, where the opposite sign of the anisotropy has been calculated.²⁴ The exact position in the phase diagram could be different among families.

Finally, the boundary between the *itinerant* and the *strong orbital differentiation* regimes shifts to lower (larger) values of the interaction with hole (electron) doping. Therefore, by changing the doping it could be possible to cross this boundary and enter a different regime. Electron doping promotes itinerancy while hole-doping can induce selective orbital localization. This is consistent with recent DMFT calculations⁴⁷ in the non-magnetic state which show a selective Mott transition of the xy orbital with hole doping. The selective localization of this orbital could had been observed already in ARPES measurements.³⁵ A change in the sign of the resistivity anisotropy in the magnetic state with hole doping has been recently reported.³⁴ Whether this is caused by hole-doping induced orbital differentiation is at present not known.

We have benefited from conversations with A. Millis, L. Boeri, I. Eremin, M. Capone, L. de Medici, and W. Ku. We acknowledge funding from MINECO-Spain through Grants FIS2008-00124 and FIS2009-08744 and FIS2011-29689.

* Electronic address: leni.bascones@icmm.csic.es

† Electronic address: belenv@icmm.csic.es

‡ Electronic address: calderon@icmm.csic.es

¹ H. Ishida and A. Liebsch, Phys. Rev. B **81**, 054513 (2010).

² P. Werner, M. Casula, T. Miyake, F. Aryasetiawan, A. J. Millis, and S. Biermann, Nature Physics **8**, 331 (2012).

³ T. Misawa, K. Nakamura, and M. Imada, Phys. Rev. Lett. **108**, 177007 (2012).

⁴ S. Raghu, X. Qi, C.-X. Liu, D. Scalapino, and S.-C. Zhang,

Phys. Rev. B **77**, 220503 (2008).

⁵ I. Mazin, M. D. Johannes, L. Boeri, and D. S. K. Koepf, Phys. Rev. B **78**, 085104 (2008).

⁶ A. Chubukov, D. Efremov, and I. Eremin, Phys. Rev. B **78**, 134512 (2008).

⁷ V. Cvetkovic and Z. Tesanovic, Europhysics Lett. **85**, 37002 (2009).

⁸ T. Yildirim, Physical Review Letters **101**, 057010 (2008).

⁹ Q. Si and E. Abrahams, Phys. Rev. Lett. **101**, 076401

- (2008).
- ¹⁰ J. Wu, P. Phillips, and A. H. Castro Neto, Phys. Rev. Lett. **101**, 126401 (2008).
 - ¹¹ L. de' Medici, S. R. Hassan, and M. Capone, Journal of Superconductivity and Novel Magnetism **22**, 535 (2009).
 - ¹² W.-G. Yin, C.-C. Lee, and W. Ku, Physical Review Letters **105**, 107004 (2010).
 - ¹³ T. Yoshida, S. Ideta, I. Nishi, A. Fujimori, M. Yi, R. G. Moore, S. K. Mo, D.-H. Lu, Z.-X. Shen, Z. Hussain, et al. (2012), arXiv:1205.6911.
 - ¹⁴ T. Sudayama, Y. Wakisaka, T. Mizokawa, S. Ibuka, R. Morinaga, T. J. Sato, M. Arita, H. Namatame, M. Taniguchi, and N. Saini (2012), arXiv:1206.2985.
 - ¹⁵ M. Aichhorn, S. Biermann, T. Miyake, A. Georges, and M. Imada, Phys. Rev. B **82**, 064504 (2010).
 - ¹⁶ Z. P. Yin, K. Haule, and G. Kotliar, Nature Physics **7**, 294 (2010).
 - ¹⁷ R. Yu and Q. Si (2012), arXiv:1202.6115.
 - ¹⁸ W. Lv, J. Wu, and P. Phillips, Phys. Rev. B **80**, 224506 (2009).
 - ¹⁹ C.-C. Lee, W.-G. Yin, and W. Ku, Phys. Rev. Lett. **103**, 267001 (2009).
 - ²⁰ E. Bascones, M. J. Calderón, and B. Valenzuela, Phys. Rev. Lett. **104**, 227201 (2010).
 - ²¹ M. Daghofer, Q.-L. Luo, R. Yu, D. X. Yao, A. Moreo, and E. Dagotto, Phys. Rev. B **81**, 180514 (2010).
 - ²² J.-H. Chu, J. G. Analytis, D. Press, K. De Greve, T. D. Ladd, Y. Yamamoto, and I. R. Fisher, Phys. Rev. B **81**, 214502 (2010).
 - ²³ M. A. Tanatar, E. C. Blomberg, A. Kreyssig, M. G. Kim, N. Ni, A. Thaler, S. L. Bud'ko, P. C. Canfield, A. I. Goldman, I. I. Mazin, et al., Phys. Rev. B **81**, 184508 (2010).
 - ²⁴ B. Valenzuela, E. Bascones, and M. J. Calderón, Phys. Rev. Lett. **105**, 207202 (2010).
 - ²⁵ C.-C. Chen, J. Maciejko, A. P. Sorini, B. Moritz, R. R. P. Singh, and T. P. Devereaux, Phys. Rev. B **82**, 100504 (2010).
 - ²⁶ A. Dusza, A. Lucarelli, F. Pfuner, J.-H. Chu, I. Fisher, and L. Degiorgi, Europhys. Lett. **93**, 37002 (2011).
 - ²⁷ J. Zhao, D. T. Adroja, D.-X. Yao, R. Bewley, S. Li, X. F. Wang, G. Wu, X. H. Chen, J. Hu, and P. Dai, Nature Physics **5**, 555 (2009).
 - ²⁸ R. R. P. Singh, arXiv:0903.4408 (2009).
 - ²⁹ T. Shimojima, K. Ishizaka, Y. Ishida, N. Katayama, K. Ohgushi, T. Kiss, M. Okawa, T. Togashi, X. Y. Wang, C. T. Chen, et al., Phys. Rev. Lett. **104**, 057002 (2010).
 - ³⁰ T.-M. Chuang, M. P. Allan, J. Lee, Y. Xie, N. Ni, S. L. Bud'ko, G. S. Boebinger, P. C. Canfield, and J. C. Davis, Science **327**, 181 (2010).
 - ³¹ M. Nakajima, T. Liang, S. Ishida, Y. Tomioka, K. Kihou, C. H. Lee, A. Iyo, H. Eisaki, T. Kakeshita, T. Ito, et al., PNAS **108**, 12238 (2011).
 - ³² W. Lv and P. Phillips, Phys. Rev. B **84**, 174512 (2011).
 - ³³ I. R. Fisher, L. Degiorgi, and Z. X. Shen, Rep. Prog. Phys. **74**, 124506 (2011).
 - ³⁴ E. C. Blomberg, M. A. Tanatar, R. M. Fernandes, B. Shen, H.-H. Wen, J. Schmalian, and R. Prozorov (2012), arXiv:1202.4430.
 - ³⁵ Talk by Z.-X. Shen in the *Materials and Mechanisms of Superconductivity* conference, Washington July 29th-August 3rd, 2012.
 - ³⁶ C. Castellani, C. R. Natoli, and J. Ranninger, Phys. Rev. B **18**, 4945 (1978).
 - ³⁷ M. J. Calderón, B. Valenzuela, and E. Bascones, Phys. Rev. B **80**, 094531 (2009).
 - ³⁸ J. Slater and G. Koster, Phys. Rev. **94**, 1498 (1954).
 - ³⁹ F. Cricchio, O. Granas, and L. Nordstrom, Phys. Rev. B **81**, 140403 (2009).
 - ⁴⁰ G.-Q. Liu, arXiv:1105.5412v1 (2011).
 - ⁴¹ T. Schikling, F. Gebhard, and J. Bünemann, Phys. Rev. Lett. **106**, 146402 (2011).
 - ⁴² M. Calderon, G. Leon, B. Valenzuela, and E. Bascones (2012), arXiv:1106.0815.
 - ⁴³ W.-G. Yin, C.-H. Lin, and W. Ku (2011), arXiv:1106.0881.
 - ⁴⁴ S. Graser, T. Maier, P. Hirschfeld, and D. Scalapino, New J. Phys. **11**, 025016 (2009).
 - ⁴⁵ Note that this is a consequence of the imposed $(\pi, 0)$ ordering. In fact, a (π, π) checkerboard magnetic order is stabilized when heavily doping with holes towards $n = 5$. See Ref.[42].
 - ⁴⁶ T. Miyake, K. Nakamura, R. Arita, and M. Imada, J. Phys. Soc. Jpn. **79**, 044705 (2010).
 - ⁴⁷ L. de' Medici, G. Giovannetti, and M. Capone (2012), unpublished.